Quassidines A−D, Bis-β-carboline Alkaloids from the Stems of *Picrasma quassioides*

Wei-Hua Jiao,[†] Hao Gao,[‡,§] Chen-Yang Li,[†] Feng Zhao,[⊥] Ren-Wang Jiang,[‡,§] Ying Wang,[‡,§] Guang-Xiong Zhou,[‡,§] and Xin-Sheng Yao*[,†,‡]

College of Traditional Chinese Materia Medica, Shenyang Pharmaceutical University, Shenyang 110016, People's Republic of China, Institute of Traditional Chinese Medicine and Natural Products, Jinan University, Guangzhou 510632, People's Republic of China, Guangdong Province Key Laboratory of Pharmacodynamic Constituents of TCM and New Drugs Research, Jinan University, Guangzhou 510632, People's Republic of China, and School of Pharmacy, Yantai University, Yantai 264005, People's Republic of China

Received September 3, 2009

Four new bis-β-carboline alkaloids, quassidines A−D (**1**−**4**), together with a known alkaloid, picrasidine C (**5**), were isolated from the stems of *Picrasma quassioides*. Quassidine A (**1**) is the first reported bis-β-carboline alkaloid possessing a novel cyclobutane moiety. The structures of the new compounds were determined on the basis of their 1D and 2D NMR and X-ray diffraction data. A possible biogenetic pathway for these alkaloids was proposed, and all compounds were evaluated for anti-inflammatory activity. Only quassidine A (**1**) showed weak activity.

Picrasma quassioides Bennet (Simaroubaceae), mainly distributed in Southern China, has been used as a traditional folk medicine for the treatment of gastroenteritis, eczema, and snakebite. In initial phytochemical work on this species, β-carbolines, canthin-6-ones, and especially bis-β-carbolines were characterized and found to exhibit potent cAMP phosphodiesterase inhibitory activity.[1−10] As part of our chemical and pharmaceutical research for bis-β-carboline alkaloids, we investigated a 95% EtOH extract of *P. quassioides* stems, which yielded an anti-inflammatory $CHCl_3$-soluble fraction (Table 1). The $CHCl_3$-soluble fraction afforded four new bis-β-carbolines, designated as quassidines A−D (**1**−**4**), together with picrasidine C (**5**). Herein, we report the isolation, structure elucidation, and possible biogenetic pathway of these alkaloids, as well as their anti-inflammatory activity.

Results and Discussion

Quassidine A (**1**) was obtained as colorless needles. Its molecular formula was established as $C_{29}H_{26}N_4O_3$ on the basis of a quasi-molecular ion peak at *m/z* 479.2108 $[M + H]^+$ in its HRESI mass spectrum. The UV spectrum of **1** displayed absorption maxima at 264, 284, and 345 nm, suggesting the presence of β-carboline moieties.[11] Its ^{1}H NMR spectrum in DMSO-d_6 (Table 1) showed signals for two methine protons (δ_H 4.81, m, H-14; δ_H 4.20, m, H-14′) and two methylene groups (δ_H 2.92, m, H-15a; δ_H 2.32, m, H-15b and δ_H 2.78, m, H-15′a; δ_H 2.16, m, H-15′b) in the upfield region. The signals of three *O*-methyl groups (δ_H 4.08, s, H_3-16 and H_3-17; δ_H 4.19, s, H_3-18) could also be observed. In addition, two aromatic singlets (δ_H 8.06, s, H-5; δ_H 8.23, s, H-5′) and two broad NH singlets (δ_H 12.64, br s, H-1; δ_H 11.51, br s, H-1′) were observed in the low-field region of the spectrum. A 1,2,3-trisubstituted aromatic ring and a 1,2-disubstituted aromatic ring were present, as evidenced by characteristic resonances (δ_H 7.72, d, J = 7.7 Hz, H-9; δ_H 7.14, t, J = 7.7 Hz, H-10; δ_H 7.07, d, J = 7.7 Hz, H-11 and δ_H 8.18, d, J = 8.0 Hz, H-9′; δ_H 7.23, td, J = 8.0, 1.0 Hz, H-10′; δ_H 7.49, td, J = 8.0, 1.0 Hz, H-11′; δ_H 7.61, d, J = 8.0 Hz, H-12′). In the ^{13}C NMR spectrum, 22 aromatic carbons of two β-carboline moieties, two tertiary carbons (δ_C 40.0, C-14; δ_C 43.7, C-14′), two secondary carbons (δ_C 20.9, C-15; δ_C 24.6, C-15′), and three *O*-methyl carbons (δ_C 56.0, C-16; δ_C 55.6, C-17; δ_C 56.1, C-18) were identified (Table 1). The two β-carboline moieties accounted for 18 of the 19 double-bond equivalents

Table 1. Inhibitory Effects of 95% Ethanol Extract and Its $CHCl_3$, EtOAc, *n*-BuOH, and H_2O Fractions on the NO Production Stimulated by LPS in Mouse Monocyte-Macrophage RAW 264.7

	inhibition (%)			
extract	100 μg/mL	30 μg/mL	10 μg/mL	3 μg/mL
95% EtOH	95.88 ± 1.74	94.20 ± 6.07	53.75 ± 6.07	9.93 ± 12.15
$CHCl_3$	96.55 ± 9.54	95.79 ± 0.85	95.48 ± 0.87	54.92 ± 4.34
EtOAc	100.00 ± 2.60	97.40 ± 6.94	43.24 ± 4.34	14.02 ± 0.87
n-BuOH	80.63 ± 2.60	59.60 ± 0.87	24.54 ± 4.34	23.95 ± 1.74
H_2O	21.04 ± 1.28	16.37 ± 1.74	15.19 ± 0.87	6.43 ± 3.47

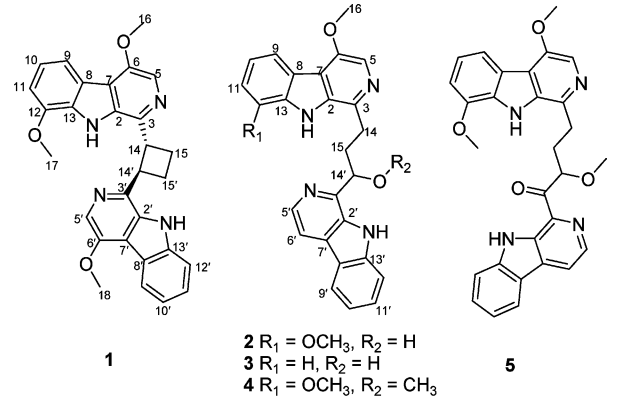

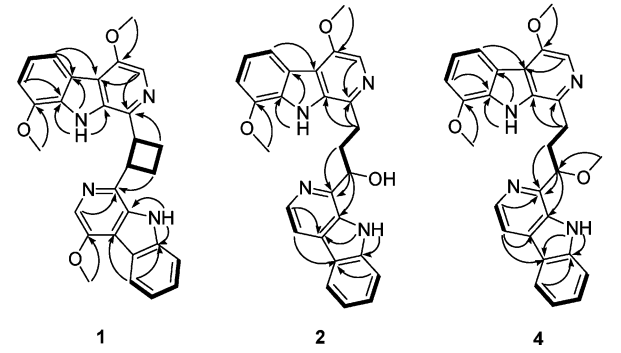

Figure 1. Key HMBC (→) and COSY (—) correlations of **1**, **2**, and **4**.

* To whom correspondence should be addressed. Tel: +86-20-85225849. Fax: +86-20-85221559. E-mail: tyaoxs@jnu.edu.cn.
† Shenyang Pharmaceutical University.
‡ Institute of Traditional Chinese Medicine and Natural Products, Jinan University.
§ Guangdong Province Key Laboratory of Pharmacodynamic Constituents of TCM and New Drugs Research, Jinan University.
⊥ Yantai University.

10.1021/np900538r
Published on Web 01/22/2010

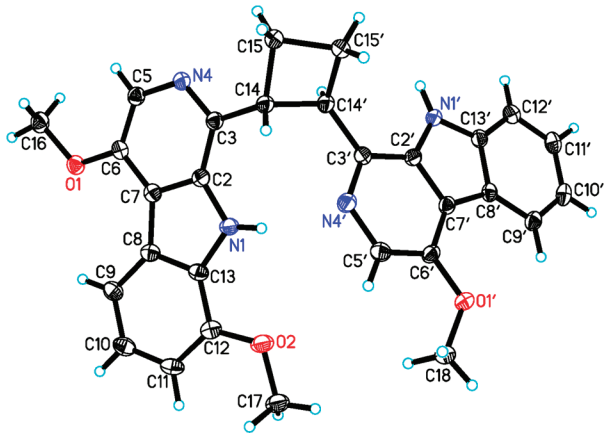

Figure 2. ORTEP drawing of quassidine A (**1**).

required by the molecular formula and indicated that **1** contained an additional ring. The complete ^{1}H and ^{13}C NMR assignments and connectivities were determined from a combination of COSY, HSQC, and HMBC data. The COSY spectrum showed correlations that indicated the connectivity of H-14, H-15a/H-15b, H-15′a/H-15′b, and H-14′, demonstrating the presence of a 1,2-disubstituted cyclobutane moiety. In the HMBC spectrum, H-15a and H-15b showed correlations to the quaternary C-3 (δ_C 140.1), while H-15′a and H-15′b showed correlations to the quaternary C-3′ (δ_C 140.6). In addition, H_3-16, H_3-17, and H_3-18 showed correlations to C-6 (δ_C 150.3), C-12 (δ_C 146.0), and C-6′ (δ_C 150.4), respectively. These correlations indicated that the two β-carboline moieties were connected to C-14 and C-14′, and the three *O*-methyl groups were located at C-6, C-12, and C-6′, confirmed by the correlations between H_3-16 and H-5, H_3-17 and H-11, and H_3-18 and H-5′ in the ROSEY experiment, respectively. The key COSY and HMBC correlations are shown in Figure 1. Furthermore, the relative configuration of **1** was established unambiguously from X-ray crystallographic analysis (Figure 2), the 6,12-dimethoxy-β-carboline moiety at C-14 existed in the α-axial orientation, and the 6-methoxy-β-carboline moiety at C-14′ existed in the β-axial orientation. Therefore, the structure of **1** was characterized as shown in Figure 2. This is the first reported bis-β-carboline alkaloid possessing a novel cyclobutane moiety.

Quassidine B (**2**) was obtained as colorless needles. Its molecular formula was established as $C_{27}H_{24}N_4O_3$ on the basis of a quasi-molecular ion peak at *m/z* 453.1920 $[M + H]^+$ in its HRESI mass spectrum. Compound **2** had a similar ^{1}H NMR spectrum to **1**, except that the resonances of the 1,2-disubstituted cyclobutane moiety and the *O*-methyl group (H_3-18) in the ^{1}H NMR spectrum of **1** were replaced by signals for a 1,3-disubstituted propan-1-ol moiety (δ_H 3.21, t, J = 7.3 Hz, H_2-14; δ_H 2.50, m, H-15a; δ_H 2.41, m, H-15b; δ_H 5.18, t, J = 7.3 Hz, H-14′) and an aromatic proton (δ_H 8.07, d, J = 5.3 Hz, H-6′). H-14 and H_2-15 were connected to two secondary carbons (δ_C 29.6, C-14; δ_C 35.4, C-15), a tertiary carbon (δ_C 72.6, C-14′), and an aromatic carbon (δ_C 113.7, C-6′) via HSQC correlations, respectively. After further analysis of the HMBC data of **2**, it was found that the methylene H_2-14 showed correlations with two quaternary carbons (δ_C 135.1, C-2; δ_C 139.6, C-3), and the oxymethine H-14′ showed correlations with two quaternary carbons (δ_C 132.8, C-2′; δ_C 147.8, C-3′). This indicated that the 6,12-dimethoxy-β-carboline moiety (part A: NH-1 to C-13) was connected to C-14 and the β-carboline moiety (part B: NH-1′ to C-13′) was connected to C-14′. The complete structure of **2** was confirmed by X-ray crystallographic analysis (Figure 3). The asymmetric unit of **2** consisted of a molecule of **2** and a molecule of MeOH connected via hydrogen bonds O4−H···N4 (D = 2.717 Å, θ = 171.7°) and O3−H···O4 (D = 2.785 Å, θ = 163.5°). The two moieties were planar with a mean deviation of 0.037 and 0.046 Å for parts A and B, respectively. Parts A and B were roughly perpendicular to each other with a dihedral angle of 94.7°. Compound **2** has a stereogenic carbon at C-14′; however, the X-ray analysis revealed that **2** exists as a racemate (space group $P\bar{1}$), which explained its specific rotation: $[\alpha]_D$ 0 (c 0.5, $CHCl_3$). Thus, the structure of **2** was determined as shown in Figure 3.

Quassidine C (**3**) was obtained as a yellowish powder. Its molecular formula was established as $C_{26}H_{22}N_4O_2$ on the basis of a quasi-molecular ion peak at *m/z* 423.1829 $[M + H]^+$ in its HRESI mass spectrum. Comparison of the ^{1}H NMR spectra of **2** and **3** showed that the two compounds were very similar, but that the *O*-methyl group (δ_H 4.04, H_3-17) that appeared in the ^{1}H NMR spectrum of **2** was replaced by an aromatic doublet (δ_H 7.61, d, J = 8.0 Hz, H-12) in the ^{1}H NMR spectrum of **3**. This was confirmed by a COSY correlation of an aromatic proton (δ_H 7.50, td, J = 8.0, 1.0 Hz, H-11) with H-12 and HMBC correlations from H-12 to carbons C-8 (δ_C 120.3) and C-10 (δ_C 119.3). The structure of **3** was assigned by a combination of 1D and 2D NMR and MS methods and by comparison with the data of **2**. Compound **3** showed no optical activity in $CHCl_3$, although it has a stereogenic C-14′; therefore, it might also exist as a racemate.

Quassidine D (**4**) was obtained as a yellowish powder. Its molecular formula was established as $C_{28}H_{26}N_4O_3$ on the basis of

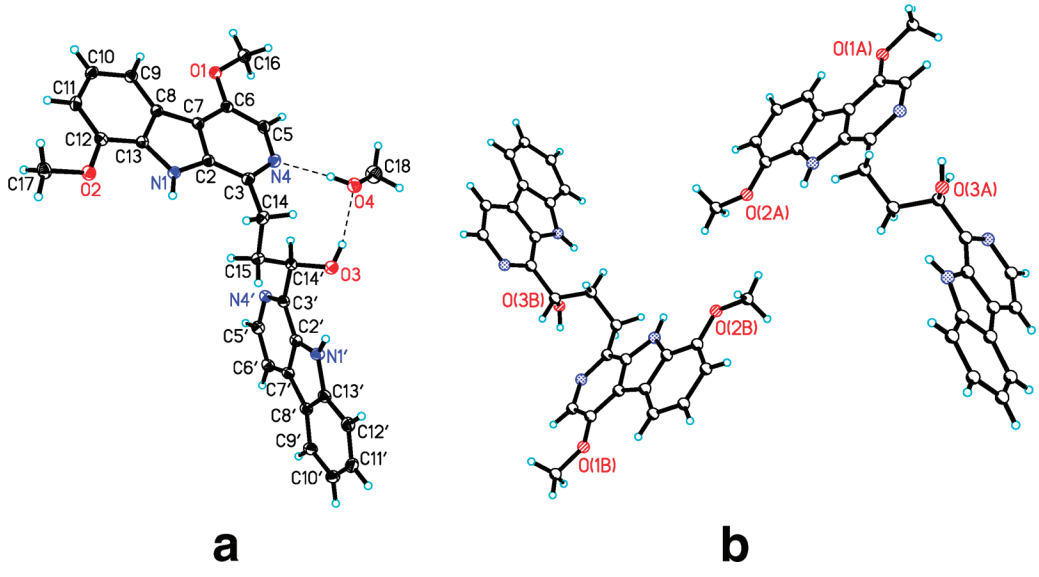

Figure 3. (a) ORTEP drawing of quassidine B (**2**). (b) Unit cell of **2** showing the 1:1 racemic complex.

Scheme 1. Possible Biogenetic Pathway for Bis-β-carboline Alkaloids

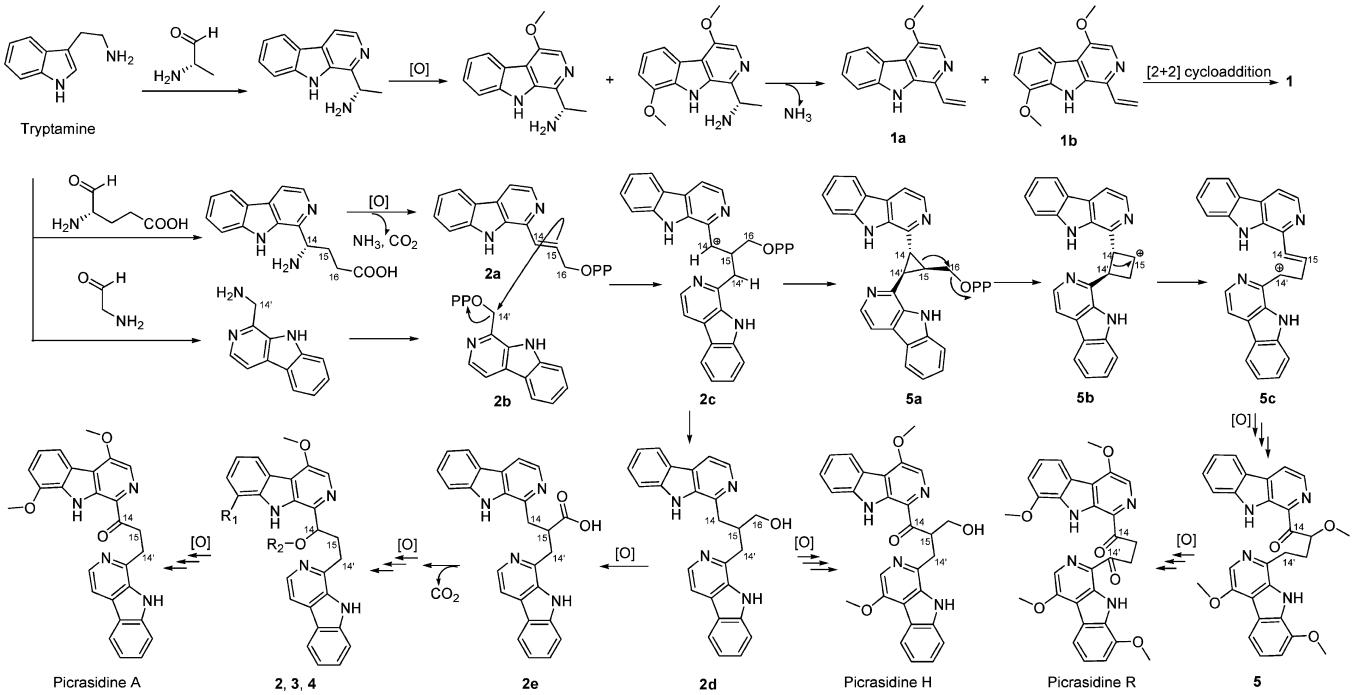

a quasi-molecular ion peak at *m/z* 467.2086 $[M + H]^+$ in its HRESI mass spectrum. Compound **4** shared similar ^1H and ^{13}C NMR spectra with **2**, although additional signals (δ_H 3.24, s, H$_3$-18; δ_C 55.8, C-18) suggested the presence of an *O*-methyl group in the structure of **4**. H$_3$-18 showed an HMBC correlation to an oxygenated methine carbon (δ_C 83.6, C-14′), and thus the *O*-methyl group was placed at position C-14′. Key COSY and HMBC correlations of **4** are shown in Figure 1. The structure of **4** was assigned by 1D and 2D NMR spectra and by comparison with the data of **2**. Compound **4** showed no optical activity in $CHCl_3$, although it has a stereogenic center C-14′; therefore, it might also exist as a racemate.

Compound **5** was found to be identical with picrasidine C, previously isolated from *P. quassioides*, by its MS and NMR data in comparison with the literature data.[2]

A possible biogenetic pathway and relationship for compounds **1**−**5** and three previously reported bis-β-carbolines (picrasidines A, H, and R) are proposed as illustrated in Scheme 1.[2,6] These bis-β-carbolines are closely related to the monomeric β-carbolines, which are derived form tryptamine condensing with other amino acids.[12] In the biogenetic pathway of **1**, compounds **1a** and **1b** might undergo a [2 + 2]-cycloaddition to form the cyclobutane moiety. In another route, precursor **2a** would condense with **2b** via an S_N2 mechanism to give the intermediate carbocation **2c**, which may be transformed into allylic cation **5c**[13] and finally lead to the formation of picrasidines C (**5**) and R.[2,6] On the other hand, pyrophosphate elimination of **2c** would give **2d** followed by selective oxidation to give picrasidine H.[6] Compound **2d** would undergo oxidation at C-16 to afford **2e**, whose decarboxylation and subsequent oxidation would finally result in the formation of compounds **2**−**4** and picrasidine A.[2]

All the isolated compounds were examined for their inhibitory effects on the production of nitric oxide (NO), tumor necrosis factor α (TNF-α), and interleukin 6 (IL-6) stimulated by LPS in mouse monocyte-macrophage RAW 264.7 (Table 3). Compound **1** showed weak inhibitory activity on NO and TNF-α production with IC_{50} values of 89.39 and 88.41 μM, respectively, which were similar to those of the positive control hydrocortisone. The inhibitory activities of **2** and **3** were not evaluated due to their potent cytotoxicity. Compounds **4** and **5** did not show any significant anti-inflammatory activity, and both had IC_{50} values greater than 100 μM.

Experimental Section

General Experimental Procedures. Optical rotations were measured with a Jasco P-1020 digital polarimeter (l = 1 cm). UV spectra were measured on a Jasco V-550 UV/vis spectrometer. IR spectra (KBr) were obtained with a Jasco FTIR-400 spectrometer. 1D and 2D NMR spectra were acquired in DMSO-d_6 or $CDCl_3$ (chemical shifts were referenced to the solvent signals) on a Bruker Avance-400 operating at 400 MHz, using an inverse probe fitted with a gradient along the *Z*-axis. ESIMS data were recorded on a Finnigan LCQ Advantage MAX spectrometer. Column chromatography (CC) was performed with Haiyang silica gel. HPLC was performed on a Gilson system with a 306 pump and a UV/vis-152 detector, using a reversed-phase column (21.2 × 250 mm, 5 μm, Welch XB-C18) at 8 mL/min and monitored at 240 nm.

Plant Material. The stems of *P. quassioides* were collected from Guangxi Autonomy, China, in June 2005 and authenticated at Guangzhou University of Traditional Chinese Medicine. A voucher specimen has been deposited at the Institute of Traditional Chinese Medicine and Natural Products, Jinan University, Guangzhou (510632), China.

Extraction and Isolation. The dried stems of *P. quassioides* (100 kg) were extracted with 95% EtOH. After filtration and evaporation of the solvent in vacuo, the resultant extract (200 g) was diluted with H_2O and then successively partitioned with $CHCl_3$, EtOAc, and *n*-BuOH three times with the same volume, to give dried $CHCl_3$-soluble (128 g), EtOAc-soluble (8.12 g), and *n*-BuOH (20.8 g) residues. The $CHCl_3$-soluble extract, which showed potent inhibitory activity on NO production stimulated by LPS in mouse monocyte-macrophage RAW 264.7 with the inhibitory ratio of 100.3% at 10 μg/mL, was subjected to silica gel column chromatography by elution with increasing concentration of EtOAc in cyclohexane to give 10 fractions (PQC1−PQC10). Fraction PQC7 (19.2 g) was subjected to silica gel column chromatography by elution with a gradient mixture of $CHCl_3$−MeOH (100:1−5:1) to give seven further fractions (1a−7a). Fraction PQC7-4a (6.0 g) was further fractionated (MPLC-ODS, stepwise, MeOH−H_2O, 10:90−100:0) to afford 10 subfractions (1−10). Subfraction PQC7-4a-10 (364.0 mg) was further fractionated by reversed-phase HPLC (MeOH−H_2O, 85:15) to afford **1** (4.5 mg, t_R 33.4 min) and **4** (6.3 mg, t_R 12.2 min). **5** (5.6 mg) was isolated from subfraction PQC7-4a-9 (210.4 mg) by Sephadex LH-20 ($CHCl_3$−MeOH, 1:1). Fraction PQC8 (6.88 g) was subjected to silica gel column chromatography by elution with a gradient mixture of $CHCl_3$−MeOH (100:1−1:1) to afford nine further fractions (1−9). **2** (154.0 mg, t_R 16.5 min) and **3** (16.8 mg, t_R 12.8 min) were obtained from fractions PQC8-7 (860.0 mg) and PQC8-9 (1.05 g) by reversed-phase HPLC (MeOH−H_2O, 80:20), respectively.

Table 2. ^{1}H NMR (400 MHz) and ^{13}C NMR (100 MHz) Data of Compounds **1**−**4**

	1[a]		**2**[a]		**3**[a]		**4**	
no.	δ_C	δ_H (J in Hz)	δ_C	δ_H (J in Hz)	δ_C	δ_H (J in Hz)	δ_C[b]	δ_H (J in Hz)[a]
1		12.64, br s		12.19, br s		11.73, br s		11.99, br s
2	134.4		135.1		134.9		136.6	
3	140.1		139.6		138.7		139.0	
5	119.7	8.06, s	119.8	7.95, s	119.8	7.95, s	119.9	7.91, s
6	150.3		149.9		149.9		151.0	
7	116.6		117.0		116.3		117.0	
8	121.4		121.5		120.3		121.2	
9	115.4	7.72, d (7.7)	115.5	7.78, d (8.0)	123.1	8.17, d (8.0)	116.4	7.75, d (8.0)
10	120.1	7.14, t (7.7)	120.0	7.16, t (8.0)	119.3	7.22, td (8.0, 1.0)	120.2	7.15, t (8.0)
11	107.0	7.07, d (7.7)	107.1	7.07, d (8.0)	126.8	7.50, td (8.0, 1.0)	106.9	7.08, d (8.0)
12	146.0		146.0		111.6	7.61, d (8.0)	146.5	
13	129.7		129.9		139.6		130.3	
14	40.0	4.81, m	29.6	3.21, t (7.3)	34.7	3.22, m	29.3	3.08, t (7.3)
15	20.9	2.92, m 2.32, m	35.4	2.50, m 2.41, m	29.3	2.50, m 2.45, m	34.6	2.49, m
1′		11.51, br s		11.37, br s		11.38, br s		11.33, br s
2′	134.0		132.8		132.7		133.0	
3′	140.6		147.8		147.9		144.7	
5′	119.0	8.23, s	136.2	8.38, d (5.3)	136.5	8.28, d (5.2)	137.2	8.35, d (5.3)
6′	150.4		113.7	8.07, d (5.3)	113.5	8.02, d (5.2)	114.4	8.09, d (5.3)
7′	116.7		128.5		128.3		131.4	
8′	120.0		120.4		120.5		122.4	
9′	123.2	8.18, d (8.0)	121.3	8.22, d (7.8)	121.3	8.21, d (7.9)	121.7	8.22, d (7.8)
10′	119.7	7.23, td (8.0, 1.0)	119.1	7.23, td (7.8, 1.0)	119.0	7.22, td (7.9, 1.0)	120.1	7.23, td (7.8, 1.0)
11′	127.1	7.49, td (8.0, 1.0)	127.9	7.54, td (7.8, 1.0)	127.8	7.53, td (7.9, 1.0)	128.8	7.54, td (7.8, 1.0)
12′	111.9	7.61, d (8.0)	112.4	7.74, d (7.8)	112.3	7.73, d (7.9)	111.8	7.70, d (7.8)
13′	139.8		140.6		140.5		140.4	
14′	43.7	4.20, m	72.6	5.18, t (7.3)	72.8	5.21, t (6.5)	83.6	4.79, t (7.3)
15′	24.6	2.78, m 2.16, m						
16	56.0	4.08, s	55.9	4.07, s	55.9	4.07, s	57.5	4.04, s
17	55.6	4.08, s	55.4	4.04, s			56.1	4.03, s
18	56.1	4.19, s					55.8	3.24, s

[a] Measured in DMSO-d_6. [b] Measured in $CDCl_3$.

Table 3. Inhibitory Effects of Compounds **1**−**5** on the NO, TNF-α, and IL-6 Production Stimulated by LPS in Mouse Monocyte-Macrophage RAW 264.7

	anti-inflammatory activity (IC_{50}, μM)		
compound	NO	TNF-α	IL-6
1	89.39	88.41	>100
2	+++[b]	+++	+++
3	+++	+++	+++
4	>100	>100	>100
5	89.91	>100	>100
hydrocortisone[a]	64.34	85.64	63.86

[a] Positive control. [b] Cytotoxity of test compound.

Bioassays. Cell Culture. Mouse monocyte-macrophage RAW 264.7 (ATCC TIB-71) was maintained in RPMI 1640 medium (Gibco) supplemented with penicillin (100 U/mL) (Gibco), streptomycin (100 μg/mL) (Gibco), and 10% heat-inactivated fetal bovine serum (Gibco) at 37 °C in a humidified incubator with 5% CO_2 and 95% air, and the medium was routinely changed every 2 days. The cells were passaged by trypsinization until they attained confluence and used for assays during the exponential growth phase.

NO Analysis and Cell Viability Assay. The RAW 264.7 cells were cultured in 96-well plates at the initial density of 5×10^5 cells/mL in RPMI 1640 medium (200 μL/well) for 1 h. The test compound or extract dissolved in DMSO at various concentrations was added (0.4 μL/well), and lipopolysaccharide (LPS) (Sigma) was also added with a final concentration of 1 μg/mL. LPS groups received LPS but not the test compound or extract, and the control groups received 0.4 μL of DMSO per well without LPS, test compound, or extract. After a 24 h incubation, the level of NO was determined by measuring the amount of nitrite in the cell culture supernatant, using Griess reagent (mixture of equal volume of reagent A and reagent B, reagent A: 1% sulfanilamide in 5% H_3PO_4, reagent B: 0.1% naphthylethylene diamine dihydrochloride). Briefly, 100 μL of the supernatant from incubates was mixed with an equal volume of Griess reagent, the absorbance at 540 nm was measured, and the inhibitory rate was calculated.[14] Cytotoxicity was determined by the mitochondrial-dependent reduction of 3-(4,5-dimethylthizaol-2-yl)-2,5-diphenyl tetrazolium bromide (MTT) (Sigma) colorimetric assay, after 24 h incubation with test compound.

Measurement of TNF-α and IL-6. The RAW 264.7 cells were cultured in 96-well plates at the initial density of 5×10^5 cells/mL in RPMI 1640 medium (200 μL/well) for 1 h. The test groups, LPS groups, and control groups were treated in the same way as the experiment for NO analysis, respectively. The cells in the 96-well plates were cultured for 6 h, and the levels of TNF-α and IL-6 in the cell culture supernatant were detected by using a mouse TNF-α enzyme-linked immunosorbent assay (ELISA) kit and a mouse IL-6 ELISA kit (R&D) according to the manufacturer's recommendations, respectively.[15]

Quassidine A (1): colorless needles ($CHCl_3$−MeOH, 1:2); mp 309 °C; $[\alpha]^{25}_D$ 0 (*c* 0.5, $CHCl_3$); UV ($CHCl_3$) λ_{max} (log ε) 246 (4.38), 284 (3.89), 334 (3.61), 345 (3.63) nm; ^{1}H and ^{13}C NMR, see Table 2; ESIMS *m/z* 479 $[M + H]^+$; HRESIMS *m/z* 479.2108 $[M + H]^+$ (cacld for $C_{29}H_{27}N_4O_3$, 479.2083).

Quassidine B (2): colorless needles ($CHCl_3$−MeOH, 1:2); mp 246 °C; $[\alpha]^{25}_D$ 0 (*c* 0.5, $CHCl_3$); UV ($CHCl_3$) λ_{max} (log ε) 245 (4.42), 288 (3.86), 348 (3.61) nm; IR (KBr) ν_{max} 3420, 1574, 1502, 1426, 739 cm^{-1}; ^{1}H and ^{13}C NMR, see Table 2; ESIMS *m/z* 453 $[M + H]^+$, 451 $[M - H]^-$; HRESIMS *m/z* 453.1920 $[M + H]^+$ (cacld for $C_{27}H_{25}N_4O_3$, 453.1927).

Quassidine C (3): yellowish powder; $[\alpha]^{25}_D$ 0 (*c* 0.5, $CHCl_3$); UV ($CHCl_3$) λ_{max} (log ε) 246 (4.37), 288 (3.99), 348 (3.65) nm; IR (KBr) ν_{max} 3219, 2848, 1733, 1716, 1625, 1567, 1541, 1507, 1456, 1297, 1061, 744 cm^{-1}; ^{1}H and ^{13}C NMR, see Table 2; ESIMS *m/z* 867 $[2M + Na]^+$, 423 $[M + H]^+$, 421 $[M - H]^-$; HRESIMS *m/z* 423.1829 $[M + H]^+$ (cacld for $C_{26}H_{23}N_4O_2$, 423.1821).

Quassidine D (4): yellowish powder; $[\alpha]^{25}_D$ 0 (*c* 0.5, $CHCl_3$); UV ($CHCl_3$) λ_{max} (log ε) 244 (4.40), 288 (3.91), 349 (3.62) nm; IR (KBr) ν_{max} 3420, 2928, 2848, 1716, 1627, 1578, 1542, 1456, 1253, 746 cm^{-1}; ^{1}H and ^{13}C NMR, see Table 2; ESIMS *m/z* 955 $[2M + Na]^+$, 467 $[M + H]^+$, 465 $[M - H]^-$; HRESIMS *m/z* 467.2086 $[M + H]^+$ (cacld for $C_{28}H_{27}N_4O_3$, 467.2083).

X-ray Crystallographic Analysis Data of 1. Colorless needles, $C_{29}H_{27}N_4O_3$, $M = 478.54$, monoclinic, $P2_1/c$, $a = 12.151(2)$ Å, $b = 8.481(1)$ Å, $c = 22.796(5)$ Å, $\gamma = 91.48(3)°$, $V = 2348.5(8)$ Å^3, $Z = 4$, $D_x = 1.353$ mg/m^3, $F(000) = 1008$, μ(Mo Kα) = 0.090 mm^{-1}. Data

collection was performed on a SMART CCD using graphite-monochromated radiation (λ = 0.71073 Å); 3354 unique reflections were collected to θ_{max} = 23.90°, in which 2404 reflections were observed [$F^2 > 4\sigma(F^2)$]. The structures were solved by direct methods (SHELXTL version 5.1) and refined by full-matrix least-squares on F^2. In the structure refinements, non-hydrogen atoms were refined anisotropically. Hydrogen atoms bonded to carbons were placed on the geometrically ideal positions by the "ride on" method. Hydrogen atoms bonded to oxygen were located by the difference Fourier method and were included in the calculation of structure factors with isotropic temperature factors. The final R = 0.0369, R_w = 0.0576, and S = 0.918.

X-ray Crystallographic Analysis Data of 2. Colorless needles, $C_{27}H_{24}N_4O_3 \cdot CH_3OH$, M = 574.52, triclinic, $P\bar{1}$, a = 6.3318(8) Å, b = 13.7667(18) Å, c = 13.9124(10) Å, α = 90.472(8)°, β = 90.815(8)°, γ = 91.818(10)°, V = 1211.9(2) Å^3, Z = 2, D_x = 1.328 mg/m^3, $F(000)$ = 512, μ(Cu Kα) = 0.09 mm^{-1}. Data collection was performed on a SMART APEX II using graphite-monochromated radiation (λ = 0.71073 Å); 2881 unique reflections were collected to θ_{max} = 26.00°, in which 2498 reflections were observed [$F^2 > 4\sigma(F^2)$]. The structures were solved by direct methods (SHELXTL version 5.1) and refined by full-matrix least-squares on F^2. In the structure refinements, non-hydrogen atoms were refined anisotropically. Hydrogen atoms bonded to carbons were placed on the geometrically ideal positions by the "ride on" method. Hydrogen atoms bonded to oxygen were located by the difference Fourier method and were included in the calculation of structure factors with isotropic temperature factors. The final R = 0.0463, R_w = 0.0527, and S = 1.059.

Acknowledgment. We thank Prof. F. P. Wang (Sichuan University) for his advice on the biogenetic pathway. The research was supported by grants from Guangzhou Municipal Science and Technology Commission (No. 2004Z1-E5011).

Supporting Information Available: Crystallographic data for the structures reported in the paper have been deposited with the Cambridge Crystallographic Data Center as supplementary publication Nos. CCDC 733534 and CCDC 733535. Copies of the data can be obtained, free of charge, on application to the Director, CCDC, 12 Union Road, Cambridge CB2 1EZ, UK (fax: +44-(0)1223-336033, or e-mail: deposit@ccdc.cam.ac.uk). This material is available free of charge via the Internet at http://pubs.acs.org.

References and Notes

(1) Ohmoto, T.; Koike, K. *Chem. Pharm. Bull.* **1982**, *30*, 1204–1209.
(2) Ohmoto, T.; Koike, K. *Chem. Pharm. Bull.* **1983**, *31*, 3198–3204.
(3) Ohmoto, T.; Koike, K.; Higuchi, T. *Chem. Pharm. Bull.* **1985**, *33*, 3356–3360.
(4) Ohmoto, T.; Koike, K. *Chem. Pharm. Bull.* **1985**, *33*, 4901–4905.
(5) Ohmoto, T.; Koike, K. *Chem. Pharm. Bull.* **1985**, *33*, 3847–3851.
(6) Koike, K.; Ohmoto, T.; Ogata, K. *Chem. Pharm. Bull.* **1986**, *34*, 2090–2093.
(7) Koike, K.; Ohmoto, T.; Higuchi, T. *Phytochemistry* **1987**, *26*, 3375–3377.
(8) Yang, J. S.; Yu, D. Q.; Liang, X. T. *Acta. Pharm. Sin.* **1988**, *23*, 267–272.
(9) Sung, Y.; Koike, K.; Nikaido, T.; Ohmoto, T.; Sankawa, U. *Chem. Pharm. Bull.* **1984**, *32*, 1872–1877.
(10) Ohmoto, T.; Nikaido, T.; Koike, K.; Kohda, K.; Sankawa, U. *Chem. Pharm. Bull.* **1988**, *36*, 4588–4592.
(11) Koike, K.; Ohmoto, T. *Chem. Pharm. Bull.* **1987**, *35*, 3305–3308.
(12) Dewick, M. P. *Medicinal Natural Products: A Biosynthetic Approach*; Wiley: Chichester, 2002; pp 349−350.
(13) Greeves, N.; Warren S. *Organic Chemistry*; Oxford University Press: Oxford, 2002; pp 1443−1444.
(14) Qiu, L.; Zhao, F.; Jiang, Z. H. *J. Nat. Prod.* **2008**, *71*, 642–646.
(15) Gao, H.; Zhao, F.; Chen, G. D. *Phytochemistry* **2009**, *70*, 795–806.

NP900538R